

Engineering and characterization of human manganese superoxide dismutase mutants with high activity and low product inhibition

Karupiah Chockalingam^{1,*}, James Luba^{2,*}, Harry S. Nick³, David N. Silverman² and Huimin Zhao¹

¹ Departments of Chemical Engineering and Biomolecular Engineering, and Chemistry, Institute for Genomic Biology, Center for Biophysics and Computational Biology, University of Illinois at Urbana-Champaign, Urbana, IL, USA

² Department of Pharmacology and Biochemistry, University of Florida, Gainesville, FL, USA

³ Department of Neuroscience, University of Florida, Gainesville, FL, USA

Keywords

directed evolution; gene therapy; kinetic analysis; product inhibition

Correspondence

D. N. Silverman, Department of Pharmacology and Biochemistry, University of Florida, Gainesville, FL 32610, USA
Fax: +1 352 392 9696
Tel: +1 352 392 3556
E-mail: Silvermn@pharmacology.ufl.edu

H. Zhao, Departments of Chemical Engineering and Biomolecular Engineering, and Chemistry, Institute for Genomic Biology, Center for Biophysics and Computational Biology, University of Illinois at Urbana-Champaign, Urbana, IL 61801, USA
Fax: +217 333 5052
Tel: +1 217 333 2631
E-mail: zhao5@uiuc.edu

*These authors contributed equally to this work

(Received 27 June 2006, revised 23 August 2006, accepted 30 August 2006)

doi:10.1111/j.1742-4658.2006.05484.x

Human manganese superoxide dismutase (hMnSOD) is a mitochondrial metalloenzyme consisting of four identical 22 kDa monomers. Each monomer has at its center a manganese (II)/(III) ion, which is surrounded in a trigonal bipyramidal arrangement by three histidine residues, one aspartate residue, and one solvent molecule. This pentameric structure is responsible for

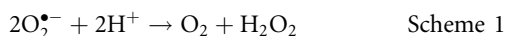
Human manganese superoxide dismutase is a mitochondrial metalloenzyme that is involved in protecting aerobic organisms against superoxide toxicity, and has been implicated in slowing tumor growth. Unfortunately, this enzyme exhibits strong product inhibition, which limits its potential biomedical applications. Previous efforts to alleviate human manganese superoxide dismutase product inhibition utilized rational protein design and site-directed mutagenesis. These efforts led to variants of human manganese superoxide dismutase at residue 143 with dramatically reduced product inhibition, but also reduced catalytic activity and efficiency. Here, we report the use of a directed evolution approach to engineer two variants of the Q143A human manganese superoxide dismutase mutant enzyme with improved catalytic activity and efficiency. Two separate activity-restoring mutations were found – C140S and N73S – that increase the catalytic efficiency of the parent Q143A human manganese superoxide dismutase enzyme by up to five-fold while maintaining low product inhibition. Interestingly, C140S is a context-dependent mutation, and the C140S–Q143A human manganese superoxide dismutase did not follow Michaelis–Menten kinetics. The re-engineered human manganese superoxide dismutase mutants should be useful for biomedical applications, and our kinetic and structural studies also provide new insights into the structure–function relationships of human manganese superoxide dismutase.

catalyzing the dismutation of the superoxide anion ($O_2^{\bullet-}$) according to the reaction in Scheme 1 below, and as such hMnSOD confers defense against superoxide toxicity [1,2]. Numerous studies have shown that MnSOD protects against reactive oxygen species-related damage resulting from cytokine treatment [3], UV light [4], irradiation [5–8], and ischemia–reperfusion

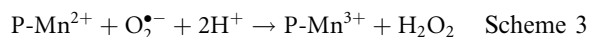
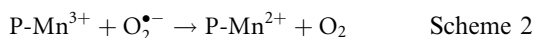
Abbreviations

FeSOD, iron superoxide dismutase; hMnSOD, human manganese superoxide dismutase; MnSOD, manganese superoxide dismutase.

[9]. In addition, although mechanistically not well understood, MnSOD has been found to play a role in the suppression of tumor growth. Several studies have shown that tumor cells/tissues contain decreased MnSOD activity [10], and other reports have indicated that restoration of MnSOD activity in transformed cancer cells (via transfection of MnSOD cDNA) results in a slowing of tumor growth in mice, as well as alteration of the transformed phenotype of cancer cells [11–17]. Given these observations, the potential role of ‘improved’ MnSODs as therapeutic agents for cancer treatment is becoming apparent [18].

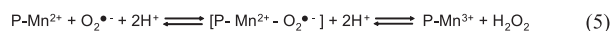
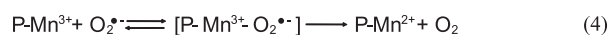


MnSOD cycles between the oxidized and reduced states, according to the reactions in Schemes 2 and 3, where P-Mn refers to the protein-bound manganese ion [19].



Studies conducted on a bacterial MnSOD using pulse radiolysis showed that this catalytic cycle is complicated by the presence of an inactive form of the enzyme that can interconvert to an active form, which manifests as an extended region of zero-order decay of superoxide following an initial burst of activity [20]. Bull *et al.* [19] later observed this inactive form spectrophotometrically during the zero-order phase of catalysis, and, on the basis of visible absorption spectra of inorganic complexes, suggested that the zero-order phase results from product inhibition by peroxide. In particular, they suggested a side-on peroxo complex of Mn(III)–SOD resulting from the oxidative addition of $\text{O}_2^{\bullet -}$ to Mn(II)–SOD. This product-inhibited complex is represented as P-Mn³⁺-X in the more complete catalytic mechanism shown in Schemes 4 and 5. Later work carried out by Silverman *et al.* [21] using stopped-flow spectrophotometry revealed that treatment of Mn(III)–SOD with excess H_2O_2 gives rise to an intermediate with a visible spectrum nearly identical to that of the inhibited enzyme during the zero-order phase of catalysis of superoxide dismutation.

Further kinetic studies in conjunction with mutational analyses conducted by Silverman and coworkers



[21–24] revealed a number of residues in the active site of hMnSOD that are important for mediating this product inhibition effect – His30, Tyr34, Gln143, and Trp161. These residues are known to be involved in an extensive hydrogen bond network surrounding the central manganese ion of each hMnSOD subunit. The function of this hydrogen bond array, although not well characterized, is thought to involve proton transfer to the peroxo-anion intermediate complex (see Scheme 5) [23].

Whereas conservative replacement of Tyr34 and Trp161 (with phenylalanine in both cases) resulted in a slower rate of zero-order decay (or an increased product inhibition effect) [21,24], certain substitutions of His30 and Gln143 were found to result in a lower extent of product inhibition than the wild-type enzyme. In particular, the His30 → Asn mutation resulted in an extent of product inhibition about four-fold lower than that of the wild-type hMnSOD, with an accompanying 10-fold drop in catalytic activity [23]. Interestingly, replacement of Gln143 with a number of different residues, even the conservative replacement with Asn, resulted in a significant drop in the extent of product inhibition [25]. In fact, all attempted replacements of Gln143 (with Ala, Val, Asn, Glu, and His) resulted in a catalytic profile whereby no zero-order phase was seen. Despite this dramatic drop in the extent of product inhibition, the Gln143 residue was also found to be critical for catalytic activity. In all the attempted replacements of Gln143, the catalytic activity (k_{cat}) of the mutant enzymes dropped by approximately two orders of magnitude. Thus, it seemed that a drop in the extent of product inhibition could not be achieved without an accompanying drop in catalytic activity.

Here, we report: (a) the development of a selection system for improving hMnSOD activity based on the ability of *Escherichia coli* to grow in the presence of the toxic compound paraquat; and (b) the use of the paraquat-based selection scheme in a directed evolution approach to identify two separate mutations that recover some of the catalytic activity lost by the imposition of the Q143A substitution. These mutations are subsequently kinetically characterized separately and in combination in the context of the parental mutant Q143A hMnSOD.

Results

Establishing the selection system

One of the key requirements in any directed evolution scheme is the development of a selection or high-

throughput screening method for the protein function of interest. In order to construct a selection system for Q143A hMnSOD mutants with enhanced catalytic activity, we took advantage of the reliance of *E. coli* on hMnSOD for survival in conditions where reactive oxygen species such as superoxide anions are present. Usually, *E. coli* has encoded within its genome its own native MnSOD and iron superoxide dismutase (FeSOD). However, an *E. coli* strain incapable of producing its own MnSOD and FeSOD, the QC774 strain, has been developed [26]. This mutant strain was used as the expression host for hMnSOD. Furthermore, to ensure that cells not producing an efficient hMnSOD enzyme did not grow, methyl viologen, or paraquat, was added to the growth media. Paraquat is known to short-circuit a portion of the respiratory electron flow in organisms, transferring electrons to O₂ to generate superoxide [27]. Note that paraquat has been previously used as a toxic agent against *E. coli* [26,28].

With this selection scheme, large libraries of protein variants could be readily screened, as most mutants of Q143A hMnSOD, presumably displaying unchanged or lower catalytic activity compared to the original Q143A hMnSOD enzyme, could not confer efficient growth to *E. coli* cells, whereas mutants with higher activity gave rise to visible, or larger, colonies on agar growth plates.

Library screening

Error-prone PCR and DNA shuffling were separately used to create a randomized library of protein variants based on the Q143A hMnSOD template. One hundred and fifty thousand QC774 transformants were screened on 40 M63 minimal media agar plates containing 1 μ M paraquat for each randomly point-mutagenized library. In addition, a control transformation was performed together with each library, whereby the plasmid expressing Q143A hMnSOD was used to transform QC774 cells, and this transformant was plated onto a 1 μ M paraquat plate so as to obtain approximately 4000 transformants. The growth (or lack of growth) of these Q143A hMnSOD-expressing cells on 1 μ M paraquat plates served as a yardstick to aid in selecting colonies on the library plates corresponding to the improved mutants.

As a relatively quick measure to ensure that the selected colonies were actually larger in size than any colony on the Q143A hMnSOD plate, each colony was grown to saturation (5–12 h) in rich (LB) medium, and dilutions (in sterile water) of these cultures were plated again on 1 μ M paraquat agar plates, so as to obtain approximately 500 colonies per plate. After

incubation of these replated mutant colonies at 37 °C for another 20–24 h, the average size of colonies on each of the mutant colony plates was compared to the average size of colonies on the Q143A hMnSOD plate by visual inspection. Mutants that clearly displayed more rapid growth than Q143A hMnSOD mutants in the paraquat-containing media were selected for further characterization, and other mutants were discarded. Plasmids from the mutants that passed this secondary screening test were isolated, and the mutant hMnSOD genes from these plasmids were amplified and reinserted into the expression vector. These re-cloned mutant plasmids were used to transform fresh QC774 *E. coli* and plated once again on 1 μ M paraquat-containing plates. This tertiary screening step helped eliminate false positives due to mutations in the bacterial chromosome or in the backbone of the expression vector. Table 1 shows the mutations present in the best mutants identified from each randomly point-mutagenized library.

Kinetic analysis

As is evident from Table 1, two mutations recurred in the mutants selected by directed evolution of Q143A hMnSOD – C140S and N73S. The catalytic constants for the C140S–Q143A hMnSOD and N73S–Q143A hMnSOD mutants obtained by directed evolution, the N73S–C140S–Q143A hMnSOD mutant created by site-directed mutagenesis, and the parent Q143A hMnSOD and wild-type hMnSOD, are given in Table 2 and Fig. 1.

Catalysis of the decay of superoxide by the single mutants of Table 2 all followed Michaelis kinetics. The single mutant C140S hMnSOD had a $k_{\text{cat}}/K_{\text{m}}$ value identical to that of wild-type hMnSOD, with evidence that product inhibition measured by $k_0/[E]$ was somewhat less than in the wild-type. In the progress curves of catalysis, an initial catalytic burst is followed by a region of zero-order decay of superoxide that is best explained by the reversible formation of an inactivated species of MnSOD [19,20]. This zero-order region predominates in the progress curves for strongly inhibited variants of MnSOD. Values of the rate constant $k_0/[E]$ for this inhibited region are obtained by fitting of expressions for the decay of superoxide to the observed progress curves [19,20]. Because of the rapid emergence of product inhibition in these measurements, we were not able to determine a value for k_{cat} . The single mutant N73S had a $k_{\text{cat}}/K_{\text{m}}$ value smaller than that of the wild-type by about two-fold, and showed product inhibition equivalent to that found in the wild-type (Table 2).

Table 1. Mutations present in 11 confirmed positive mutants obtained from screening of libraries generated by random mutagenesis (error-prone PCR and DNA shuffling) of the Q143A hMnSOD gene. Amino acid substitutions (capital letters) and base pair substitutions (small letters) are indicated. Recurring amino acid substitutions are indicated by bold type.

Mutants obtained from error-prone PCR		Mutants obtained from DNA shuffling	
Mutant	Mutations	Mutant	Mutations
EP-2	E42V (a → t), C140S (t → a), Q143A (cag → gcg), E187Q (g → c)	DS-2	C140S (t → a), Q143A (cag → gcg)
EP-15	A50V (c → t), C140S (t → a), Q143A (cag → gcg)	DS-9	L14 (g → a), N73S (a → g), Q143A (cag → gcg)
EP-40	C140S (t → a), Q143A (cag → gcg)	DS-10	N73S (a → g), K98 (a → g), Q143A (cag → gcg), D159 (t → c)
EP-46	N129D (a → g), C140S (t → a), Q143A (cag → gcg)	DS-11	K1N (g → t), P16 (t → c), C140S (g → c), Q143A (cag → gcg)
EP-59	K90T (a → c), C140S (t → a), Q143A (cag → gcg)	DS-14	K44R (a → g), C140S (t → a), Q143A (cag → gcg)
		DS-20	L60 (t → c), N73S (a → g), Q143A (cag → gcg)

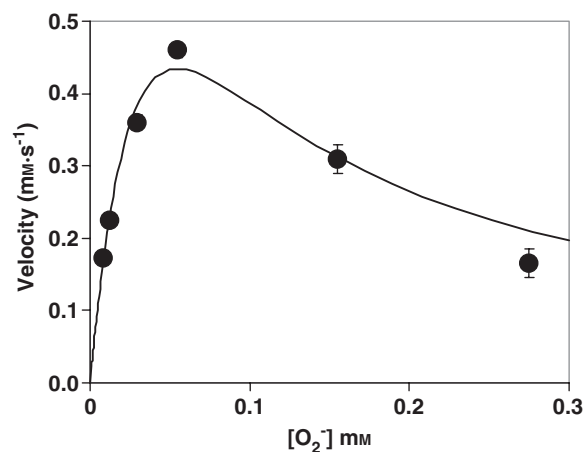
Table 2. Steady-state constants and rate constant for product inhibition $k_0/[E]$ for the decay of superoxide catalyzed by wild-type hMnSOD and mutants.

Enzyme	k_{cat}/K_m ($\mu\text{M}^{-1}\cdot\text{s}^{-1}$)	k_{cat} (ms^{-1})	$k_0/[E]$ (s^{-1})
Wild-type ^a	800	40	500
C140S ^b	800	– ^e	1000
N73S ^b	470	– ^e	500
Q143A ^c	3.1	0.50	– ^f
N73S–Q143A ^d	13	0.75	– ^f
N73S–C140S–Q143A ^d	15	1.3	– ^f

^a From Hsu *et al.* [29] and Hearn *et al.* [30]. ^b Measured at pH 8.0 by pulse radiolysis. ^c From Leveque *et al.* [25]. ^d Measured at pH 9.0 by stopped-flow spectrophotometry. ^e Catalysis was too rapid and product inhibition too strong for these values to be determined by stopped-flow spectrophotometry. ^f These mutants had a very small extent of inhibition.

Catalysis of the decay of superoxide by N73S–Q143A hMnSOD and N73S–C140S–Q143A hMnSOD showed that directed evolution was successful in identifying mutations that enhance the efficiency of catalysis compared with Q143A hMnSOD: each had k_{cat}/K_m values enhanced by approximately four-fold to five-fold (Table 2). For these mutants, the rate of catalysis was still low compared with the wild-type, and no appreciable product inhibition was measured.

Catalysis by the double mutant C140S–Q143A hMnSOD did not follow Michaelis kinetics. Initial velocities reached a maximum and then decreased at higher substrate concentrations (Fig. 1). This apparent inhibition at higher substrate concentrations was not observed in initial velocity studies of wild-type hMnSOD [29], Q143A hMnSOD [25], or the other mutants in Table 2. Product inhibition has been shown to be a prominent feature of catalysis by wild-type hMnSOD [19–21] and site-specific mutants of hMnSOD [30]. However, product inhibition is so weak in mutants in

**Fig. 1.** The initial velocity of the decay of superoxide catalyzed by C140S–Q143A hMnSOD as a function of superoxide concentration. Data were obtained by using stopped-flow spectrophotometry to measure the absorbance of superoxide at 250 nm. Solutions contained 100 mM Ches, 1.0 mM Taps, 0.5 mM EDTA, and 4.5 vol.% dimethylsulfoxide at pH 9.0 and 25 °C, with enzyme present at 20 μM . Each point represents the average of at least seven measurements. The solid line is a least-square fit of Eqn (1) to the data, resulting in: $k_{\text{cat}}/K_m = 1.2 \mu\text{M}^{-1}\cdot\text{s}^{-1}$; $k_{\text{cat}} = 0.6 \text{ ms}^{-1}$; and $K_I = 0.06 \text{ mM}$.

which Gln143 is replaced that it is difficult to observe [22,25]. Hence, we do not attribute the decrease in activity at high substrate concentrations observed for the mutant C140S–Q143A hMnSOD to product inhibition. Instead, we have used an expression describing substrate inhibition to fit the data of Fig. 1. This expression (Eqn 1) contains an inhibition constant K_I for substrate as an uncompetitive inhibitor [31]; moreover, it contains the known rate constant, k_{uncat} , for the uncatalyzed dismutation of superoxide [32]. A least-square fit of Eqn (1) to the data of Fig. 1 yields the constants given in the legend of Fig. 1. The values of k_{cat}/K_m and k_{cat} for catalysis by C140S–

Q143A hMnSOD were independent of pH in the pH range 8.0–10.5.

$$v = k_{\text{uncat}}[\text{O}_2^{\bullet-}]^2 + k_{\text{cat}}[\text{E}][\text{O}_2^{\bullet-}]/\{K_m + [\text{O}_2^{\bullet-}] + [\text{O}_2^{\bullet-}]^2/K_1\} \quad (1)$$

Because we are uncertain of the cause of the non-Michaelian behavior of C140S–Q143A hMnSOD, we have not placed these derived constants in Table 2. Data for the C140S–Q143A hMnSOD mutant can be found in Fig. 1.

Discussion

Among the replacements of active site residues in hMnSOD that do not include the first-shell ligands, the replacement of Gln143 causes the most extensive changes in catalysis [33]. The side chain carboxamide of Gln143 forms a hydrogen bond with the manganese-bound solvent molecule and participates in a hydrogen-bonded network of side chains and solvent molecules that extends to the adjacent subunit [34]. The replacement of Gln143 by Ala causes a substantial decrease, by about two orders of magnitude, in the steady-state constants for catalysis, as shown in Table 2. This probably occurs through breaking of the hydrogen bond network and by alteration in the redox potential at the active site [22,25,35]. It is notable that directed evolution has revealed mutations of human MnSOD that reverse this effect (Table 2).

Although the single replacement N73S does not enhance activity, this replacement in the double mutant N73S–Q143A causes an increase in catalysis (Table 2). Based on the kinetic data in Table 2 and an analysis of the X-ray crystal structure of hMnSOD (PDB code: 1N0J) (Fig. 2), it is evident that the N73S substitution may directly affect catalysis through an interaction with the side chain of Gln143. Table 2 suggests that the Asn73 residue contributes to enzymatic activity, as the catalytic efficiency of the enzyme drops by 41% after substitution of Asn with Ser in the context of the wild-type enzyme. This may, at least in part, be due to a loss of the interaction between the side chains of Asn73 and Gln143. The X-ray crystal structure of hMnSOD shows that the side chain amide of Asn73 is near to (3.1 Å) and possibly hydrogen bonded with the side chain carbonyl of Gln143. With the substitution of Gln143 with Ala, this favorable interaction between Gln143 and Asn73 would be disrupted. It is possible that the N73S substitution reorients the Q143A-containing active site so that it carries out catalysis more efficiently. This reorientation probably occurs through an indirect route, as both muta-



Fig. 2. X-ray crystal structure (PDB Code: 1N0J) of one monomer of wild-hMnSOD showing the relative positions of the residues that were changed in positive mutants obtained by directed evolution of Q143A hMnSOD. Two mutations, C140S and N73S, were found separately that are thought to play an important role in altering the function of Q143A hMnSOD to better protect QC774 *E. coli* cells from superoxide toxicity.

tions result in a shorter side chain, decreasing the likelihood of a direct interaction.

It is worth noting that N73S–Q143A hMnSOD has a low level of product inhibition, similar to that of the parent mutant Q143A hMnSOD, while exhibiting higher catalytic activity and efficiency. Although even higher catalytic activity would have been desirable, this result demonstrates that our directed evolution approach can indeed be used to engineer mutant enzymes with higher catalytic activities, and similarly low levels of product inhibition, relative to the parent enzyme.

It is difficult to comment on C140S–Q143A hMnSOD, as its catalysis is non-Michaelian (Fig. 1). If we accept the substrate inhibition model of Eqn (1), then the catalysis by this double mutant is less efficient than that of Q143A hMnSOD (Table 2). Interestingly, introducing the replacement N73S produces the triple mutant N73S–C140S–Q143A hMnSOD, which exhibits Michaelian behavior with negligible product inhibition; this more closely resembles the catalytic behavior of N73S–Q143A hMnSOD (Table 2). This observation suggests that the N73S substitution plays a stronger role in dictating the mode of catalytic action than the C140S mutation when they are introduced simultaneously into the Q143A hMnSOD mutant enzyme. In

fact, the catalytic efficiency of the triple mutant N73S–C140S–Q143A hMnSOD is essentially the same as that of N73S–Q143A hMnSOD.

Cys140 has its C α located 12.5 Å from the manganese, with its side chain pointing away from the manganese and buried, not exposed to bulk solvent [34]. There are no apparent hydrogen bonds involving the side chain of Cys140 and adjacent residues; it is probably hydrogen bonded with buried water molecules that are not seen in the crystal structure. However, the backbone amide and carbonyl of Cys140 form hydrogen bonds with the backbone carbonyl and amide of Trp123, the side chain of which forms one wall of the active site cavity and the replacement of which decreases catalytic activity [36]. This suggests a mechanism by which the replacement of Cys140 could alter catalytic activity.

The reason for the different mode of catalytic action of mutant C140S–Q143A hMnSOD relative to the other variants of hMnSOD containing the mutations Q143A, C140S and N73S (Table 2 and Fig. 1) is not immediately clear. The data appear consistent with substrate inhibition, but other explanations are possible. X-ray crystal structures of the various mutants may further enhance our understanding of the structural/mechanistic contribution of the various mutations, and current efforts are focused in this direction.

The engineering of increased catalytic activity or efficiency in enzymes is a significant challenge in protein engineering, but was made possible here, particularly in the N73S–Q143A hMnSOD mutant, through the careful setup and implementation of a selection system based on the resistance of *E. coli* to superoxide toxicity. It may well be questioned as to why, even though wild-type hMnSOD leads to more rapid growth of QC774 *E. coli* under superoxide pressure, the wild-type hMnSOD was not reverted to in our directed evolution libraries based on the Q143A hMnSOD mutant. The simplest explanation for this observation is that two simultaneous base pair substitutions in the codon for residue 143 would be required to revert from Gln to Ala, making this substitution highly improbable in a point-mutagenized library.

It should be pointed out that, given the success of our selection system in identifying improved hMnSOD variants, mutagenesis approaches other than the random mutagenesis approaches of error-prone PCR and DNA shuffling could be potentially used to create libraries of hMnSOD variants for selection. For example, mutagenesis could be focused on functionally important regions such as the active site or hydrogen bond network, in a manner similar to a mutagenesis strategy that we have used previously [37]. Other approaches,

such as family shuffling [38] of MnSOD members from different organisms, could also be used to create new MnSOD-based diversity.

An interesting finding of this work is the observation that the C140S mutation is present only in the enzyme variant library created by error-prone PCR-based mutagenesis, whereas both the C140S and N73S mutations were found in the library created by DNA shuffling mutagenesis. DNA shuffling mutagenesis may thus be able to access mutations that error-prone PCR cannot access. One possible origin for this difference may be the differing degrees of secondary structure formation between DNA shuffling and error-prone PCR, which utilize different-sized template DNA molecules.

Conclusions

By linking hMnSOD activity to the growth of *E. coli* QC774 cells in paraquat-containing minimal media, we have developed a convenient method for selecting mutants with increased catalytic activity from a large library of hMnSOD variants. In particular, the application of the random mutagenesis methods of error-prone PCR and DNA shuffling to the catalytically deprived, product-uninhibited Q143A hMnSOD mutant template, followed by selection, led to the identification of two mutants that confer enhanced survival ability to *E. coli* in paraquat-containing media. The mutation N73S was found to be particularly important for restoring some catalytic activity. The Q143A–C140S hMnSOD had a catalytic mechanism that differed from the Michaelian behavior of the parent, Q143A hMnSOD. The N73S–Q143A hMnSOD mutant exhibited higher catalytic efficiency and similarly low product inhibition compared with the Q143A hMnSOD parent. Our results demonstrate the ability of directed evolution to engineer variants of hMnSOD with high catalytic activity and low product inhibition. Such hMnSOD variants could be useful agents in cancer therapy.

Experimental procedures

Reagents and kits

All plasmids from *E. coli* were purified with the QIAprep spin plasmid miniprep kit (Qiagen, Chatsworth, CA). All agarose gels used contained 1% agarose. Gel extractions of DNA from agarose gels were performed with the QIAEX II gel purification kit (Qiagen). Purification of standard PCR products from other components of the reaction mixture was performed with the QIAquick PCR purification kit (Qiagen). All restriction enzymes, as well as T4 DNA ligase, were purchased from New England Biolabs (Beverly, MA).

Taq DNA polymerase was obtained from Promega (Madison, WI), and Turbo *Pfu* DNA polymerase was purchased from Stratagene (La Jolla, CA). Unless otherwise specified, all other reagents were obtained from Sigma-Aldrich (St Louis, MO).

Plasmids, strains, and subcloning

The pTrc99A vector (Amersham Pharmacia Biotech, Piscataway, NJ), QC774 *E. coli* strain (GC4468 Φ (*sodA-lacZ*)49 Φ (*sodB-kan*)1- Δ_2 Cm^r Km^r) and pTrc99A constructs expressing wild-type hMnSOD, Q143A hMnSOD and H30N hMnSOD are described elsewhere [30]. The pTrc99A vector was prepared for subcloning of the hMnSOD gene by removing a 40 bp fragment from the multiple cloning site of the vector by digestion with *NcoI* and *PstI*. This vector backbone was excised from an agarose gel and purified. For both standard and error-prone PCR amplification of hMnSOD genes, the following primers were used: hMnSOD5B, 5'-CACAGGAAACAGATCATGAAG-3'; and hMnSOD3P, 5'-CAAGCTTGCATGCCTGCAGT-3'. hMnSOD5B incorporates a recognition site for the restriction enzyme *BspHI*, and hMnSOD3P contains a recognition site for *PstI*. hMnSOD genes amplified with these two primers were first purified (using the QIAquick PCR purification kit for standard PCR products, or using the QIAEX II gel purification kit for error-prone PCR products), and then digested with both *BspHI* and *PstI*. After subsequent purification of the digested hMnSOD gene using the QIAquick PCR purification kit, the product was ligated into the pTrc99A backbone created by *NcoI*-*PstI* digestion.

Growth media

Rich medium was LB medium (Becton-Dickinson, Franklin Lakes, NJ). M63 minimal media, made according to Miller [39], was supplemented with 1 $\mu\text{g}\cdot\text{mL}^{-1}$ thiamine, as well as 0.5 mM of each of the amino acids L-isoleucine, L-leucine and L-valine. For paraquat-containing media, filter-sterilized methyl viologen in the appropriately concentrated stock solution was added to the growth media after autoclaving and brief cooling, resulting in a 1000-fold dilution of the stock solution.

Error-prone PCR and DNA shuffling

The error-prone PCR reaction contained (100 μL final volume): 10 mM Tris/HCl (pH 8.3 at 25 °C), 50 mM KCl, 7 mM MgCl₂, 0.01% (w/v) gelatine, 0.2 mM dGTP, 0.2 mM dATP, 1 mM dCTP, 1 mM dTTP, 0.10 mM MnCl₂, 0.5 μM both primers, 10 ng of template plasmid, and 5 U of *Taq* DNA polymerase. Error-prone PCR was performed in an MJ Research (Watertown, MA) PTC-200 thermocycler for 15 cycles: 1 min at 94 °C, 1 min at 50 °C, and 1 min at

72 °C. The PCR products were gel-purified, and this was followed by restriction digestion with *BspHI* and *PstI* and subcloning into the pTrc99A plasmid backbone created by *NcoI*/*PstI* digestion. Salts were removed from ligation reactions by precipitating the ligated DNA with *n*-butanol, as described previously [40], prior to transformation of the ligated libraries into QC774 *E. coli* by electroporation. DNA shuffling was performed essentially as described in Zhao and Arnold [41], except that *Taq* polymerase was the only DNA polymerase used for the reassembly of DNase I-digested fragments, whereas an equal number of units of both *Taq* and *Pfu* DNA polymerases were used for the amplification of the reassembled product.

Preparation of enzymes

The expression vectors containing C140S-Q143A and N73S-Q143A hMnSOD cDNA were transformed into the *sodA*⁻/*sodB*⁻ null mutant *E. coli* strain QC774 [26]. The bacterial growth medium was supplemented with 0.6 mM MnCl₂. Cells were gathered by centrifugation, lysed, heated to 60 °C, and then extensively dialyzed against buffer. Purification was achieved using FPLC on a Q-Sepharose anion-exchange resin (Amersham Pharmacia Biotech) and by gel filtration on a Sephacryl S-300 column (GE Healthcare Bio-Sciences, Piscataway, NJ). SDS/PAGE showed one intense band at 22 kDa. The protein concentration was determined spectrophotometrically ($\epsilon_{280} = 40\,500\text{ M}^{-1}\cdot\text{cm}^{-1}$). The enzyme concentration was set at the total manganese concentration determined by atomic absorption spectroscopy.

Catalysis

Steady-state constants for the decay of superoxide caused by mutants of hMnSOD were measured by stopped-flow spectrophotometry (Applied Photophysics SX18.MV, Leatherhead, Surrey) based on the method of McClune and Fee [42] as modified by Greenleaf *et al.* [36] and by pulse radiolysis as described by Cabelli *et al.* [24]. Potassium superoxide was dissolved in dry dimethylsulfoxide with the solution enhanced with 18-crown-6 ether. In a dual mixing experiment, this solution was diluted 10-fold with an aqueous solution of 2.0 mM Taps and 1.0 mM EDTA at pH 11. After a 0.5 s delay, this superoxide solution was mixed 1 : 1 (v/v) with buffered enzyme solution. Final solutions after mixing contained 0.5 mM EDTA, 1.0 mM Taps, DMSO at 4.5 vol.%, and 100 mM of one of the following buffers: Taps (pH 8.0–8.5); Ches (pH 9.0–9.5); and Taps (pH 10.0–10.5). The superoxide concentration was varied from approximately 0.01 mM to 0.6 mM, and the enzyme concentrations were near 20 μM . The change in absorbance of superoxide was measured at 250 nm ($\epsilon_{250} = 2000\text{ M}^{-1}\cdot\text{cm}^{-1}$) [43]. Initial velocities were determined from the first 5–10% of the reaction.

Acknowledgements

This work was supported by NIH grant GM54903 (DS) and National Science Foundation CAREER Award Bes-0348107 (HZ). We thank Patrick Quint and Diane Cabelli for help with kinetics, and Chingkuang Tu for assistance and helpful discussion. We are grateful to Max Iurcovich for excellent technical assistance.

References

- Lebovitz RM, Zhang HJ, Vogel H, Cartwright J, Dionne L, Lu NF, Huang S & Matzuk MM (1996) Neurodegeneration, myocardial injury, and perinatal death in mitochondrial superoxide dismutase-deficient mice. *Proc Natl Acad Sci USA* **93**, 9782–9787.
- Li YB, Huang TT, Carlson EJ, Melov S, Ursell PC, Olson TL, Noble LJ, Yoshimura MP, Berger C, Chan PH *et al.* (1995) Dilated cardiomyopathy and neonatal lethality in mutant mice lacking manganese superoxide dismutase. *Nat Genet* **11**, 376–381.
- Liu RG, Buettner GR & Oberley LW (2000) Oxygen free radicals mediate the induction of manganese superoxide dismutase gene expression by TNF- α . *Free Radic Biol Med* **28**, 1197–1205.
- Poswig A, Wenk J, Brenneisen P, Wlaschek M, Hommel C, Quel G, Faisst K, Dissemond J, Briviba K, Krieg T *et al.* (1999) Adaptive antioxidant response of manganese superoxide dismutase following repetitive UVA irradiation. *J Invest Dermatol* **112**, 13–18.
- Epperly MW, Bray JA, Krager S, Berry LM, Gooding W, Engelhardt JF, Zwacka R, Travis EL & Greenberger JS (1999) Intratracheal injection of adenovirus containing the human MnSOD transgene protects athymic nude mice from irradiation-induced organizing alveolitis. *Int J Radiat Oncol Biol Phys* **43**, 169–181.
- Stickle RL, Epperly MW, Klein E, Bray JA & Greenberger JS (1999) Prevention of irradiation-induced esophagitis by plasmid/liposome delivery of the human manganese superoxide dismutase transgene. *Radiat Oncol Invest* **7**, 204–217.
- Epperly MW, Sikora C, Defilippi S, Bray J, Koe G, Liggitt D, Luketich JD & Greenberger JS (2000) Plasmid/liposome transfer of the human manganese superoxide dismutase transgene prevents ionizing irradiation-induced apoptosis in human esophagus organ explant culture. *Int J Cancer* **90**, 128–137.
- Kanai AJ, Zeidel ML, Lavelle JP, Greenberger JS, Birder LA, De Groat WC, Apodaca GL, Meyers SA, Ramage R & Epperly MW (2002) Manganese superoxide dismutase gene therapy protects against irradiation-induced cystitis. *Am J Physiol Renal Physiol* **283**, F1304–F1312.
- Dobashi K, Ghosh B, Orak JK, Singh I & Singh AK (2000) Kidney ischemia–reperfusion: modulation of antioxidant defenses. *Mol Cell Biochem* **205**, 1–11.
- Wang LI, Miller DP, Sai Y, Liu G, Su L, Wain JC, Lynch TJ & Christiani DC (2001) Manganese superoxide dismutase alanine-to-valine polymorphism at codon 16 and lung cancer risk. *J Natl Cancer I*, 1818–1821.
- Church SL, Grant JW, Ridnour LA, Oberley LW, Swanson PE, Meltzer PS & Trent JM (1993) Increased manganese superoxide dismutase expression suppresses the malignant phenotype of human melanoma cells. *Proc Natl Acad Sci USA* **90**, 3113–3117.
- Li JJ, Oberley LW, St Clair DK, Ridnour LA & Oberley TD (1995) Phenotypic changes induced in human breast cancer cells by overexpression of manganese-containing superoxide dismutase. *Oncogene* **10**, 1989–2000.
- Lam EWN, Zwacka R, Engelhardt JF, Davidson BL, Domann FE, Yan T & Oberley LW (1997) Adenovirus-mediated manganese superoxide dismutase gene transfer to hamster cheek pouch carcinoma cells. *Cancer Res* **57**, 5550–5556.
- Li N, Oberley TD, Oberley LW & Zhong WX (1998) Overexpression of manganese superoxide dismutase in DU145 human prostate carcinoma cells has multiple effects on cell phenotype. *Prostate* **35**, 221–233.
- Yan T, Oberley LW, Zhong WX & St Clair DK (1996) Manganese-containing superoxide dismutase overexpression causes phenotypic reversion in SV40-transformed human lung fibroblasts. *Cancer Res* **56**, 2864–2871.
- Liu RG, Oberley TD & Oberley LW (1997) Transfection and expression of MnSOD cDNA decreases tumor malignancy of human oral squamous carcinoma SCC-25 cells. *Hum Gene Ther* **8**, 585–595.
- Zhong WX, Oberley LW, Oberley TD & St Clair DK (1997) Suppression of the malignant phenotype of human glioma cells by overexpression of manganese superoxide dismutase. *Oncogene* **14**, 481–490.
- Davis CA, Hearn AS, Fletcher B, Bickford J, Garcia JE, Leveque V, Melendez JA, Silverman DN, Zucali J, Agarwal A *et al.* (2004) Potent anti-tumor effects of an active site mutant of human manganese-superoxide dismutase. Evolutionary conservation of product inhibition. *J Biol Chem* **279**, 12769–12776.
- Bull C, Niederhoffer EC, Yoshida T & Fee JA (1991) Kinetic studies of superoxide dismutases – properties of the manganese containing protein from *Thermus thermophilus*. *J Am Chem Soc* **113**, 4069–4076.
- McAdam ME, Fox RA, Lavelle F & Fielden EM (1977) A pulse-radiolysis study of the manganese-containing superoxide dismutase from *Bacillus stearothermophilus*: a kinetic model for the enzyme action. *Biochem J* **165**, 71–79.
- Hearn AS, Tu C, Nick HS & Silverman DN (1999) Characterization of the product-inhibited complex in

- catalysis by human manganese superoxide dismutase. *J Biol Chem* **274**, 24457–24460.
- 22 Hsieh Y, Guan Y, Tu C, Bratt PJ, Angerhofer A, Lepock JR, Hickey MJ, Tainer JA, Nick HS & Silverman DN (1998) Probing the active site of human manganese superoxide dismutase: the role of glutamine 143. *Biochemistry* **37**, 4731–4739.
- 23 Ramilo CA, Leveque V, Guan Y, Lepock JR, Tainer JA, Nick HS & Silverman DN (1999) Interrupting the hydrogen bond network at the active site of human manganese superoxide dismutase. *J Biol Chem* **274**, 27711–27716.
- 24 Cabelli DE, Guan Y, Leveque V, Hearn AS, Tainer JA, Nick HS & Silverman DN (1999) Role of tryptophan 161 in catalysis by human manganese superoxide dismutase. *Biochemistry* **38**, 11686–11692.
- 25 Leveque VJ, Stroupe ME, Lepock JR, Cabelli DE, Tainer JA, Nick HS & Silverman DN (2000) Multiple replacements of glutamine 143 in human manganese superoxide dismutase: effects on structure, stability, and catalysis. *Biochemistry* **39**, 7131–7137.
- 26 Carlouz A & Touati D (1986) Isolation of superoxide dismutase mutants in *Escherichia coli*: is superoxide dismutase necessary for aerobic life? *EMBO J* **5**, 623–630.
- 27 Gao BF, Flores SC, Bose SK & McCord JM (1996) A novel *Escherichia coli* vector for oxygen-inducible high level expression of foreign genes. *Gene* **176**, 269–272.
- 28 Morimyo M, Hongo E, Hamainaba H & Machida I (1992) Cloning and characterization of the *mvrC* gene of *Escherichia coli* K-12 which confers resistance against methyl viologen toxicity. *Nucleic Acids Res* **20**, 3159–3165.
- 29 Hsu JL, Hsieh Y, Tu C, O'Connor D, Nick HS & Silverman DN (1996) Catalytic properties of human manganese superoxide dismutase. *J Biol Chem* **271**, 17687–17691.
- 30 Hearn AS, Stroupe ME, Cabelli DE, Lepock JR, Tainer JA, Nick HS & Silverman DN (2001) Kinetic analysis of product inhibition in human manganese superoxide dismutase. *Biochemistry* **40**, 12051–12058.
- 31 Cornish-Bowden A (1995) *Fundamentals of Enzyme Kinetics*. 2nd edn, pp. 121–122. Portland Press Ltd., London.
- 32 Marklund S (1976) Spectrophotometric study of spontaneous disproportionation of superoxide anion radical and sensitive direct assay for superoxide dismutase. *J Biol Chem* **251**, 7504–7507.
- 33 Silverman DN & Nick HS (2002) Catalytic pathway of manganese superoxide dismutase by direct observation of superoxide. *Methods Enzymol* **349**, 61–74.
- 34 Borgstahl GEO, Pokross M, Chehab R, Sekher A & Snell EH (2000) Cryo-trapping the six-coordinate, distorted-octahedral active site of manganese superoxide dismutase. *J Mol Biol* **296**, 951–959.
- 35 Maliekal J, Karapetian A, Vance C, Yikilmaz E, Wu Q, Jackson T, Brunold TC, Spiro TG & Miller AF (2002) Comparison and contrasts between the active site PKs of Mn-superoxide dismutase and those of Fe-superoxide dismutase. *J Am Chem Soc* **124**, 15064–15075.
- 36 Greenleaf WB, Perry JJ, Hearn AS, Cabelli DE, Lepock JR, Stroupe ME, Tainer JA, Nick HS & Silverman DN (2004) Role of hydrogen bonding in the active site of human manganese superoxide dismutase. *Biochemistry* **43**, 7038–7045.
- 37 Chockalingam K, Chen ZL, Katzenellenbogen JA & Zhao HM (2005) Directed evolution of specific receptor–ligand pairs for use in the creation of gene switches. *Proc Natl Acad Sci USA* **102**, 5691–5696.
- 38 Cramer A, Raillard SA, Bermudez E & Stemmer WP (1998) DNA shuffling of a family of genes from diverse species accelerates directed evolution. *Nature* **391**, 288–291.
- 39 Miller JH (1972) *Experiments in Molecular Genetics*. Cold Spring Harbor Laboratory Press, Cold Spring Harbor.
- 40 Thomas MR (1994) Simple, effective cleanup of DNA ligation reactions prior to electrotransformation of *Escherichia coli*. *Biotechniques* **16**, 988–990.
- 41 Zhao H & Arnold FH (1997) Optimization of DNA shuffling for high fidelity recombination. *Nucleic Acids Res* **25**, 1307–1308.
- 42 McClune GJ & Fee JA (1978) A simple system for mixing miscible organic solvents with water in 10–20 ms for the study of superoxide chemistry by stopped-flow methods. *Biophys J* **24**, 65–69.
- 43 Rabani J & Nielson SO (1969) Absorption spectrum and decay kinetics of O_2^- and HO_2 in aqueous solutions by pulse radiolysis. *J Phys Chem* **73**, 3736–3744.